

1 **A reconstruction of annual mass balances of** 2 **Austria's glaciers from 1969 to 1998**

3

4 **J. Abermann^{1,2} M. Kuhn^{2,1} and A. Fischer²**

5

6 ¹Austrian Academy of Sciences, Commission for Geophysical Research, Vienna, Austria

7 ²Institute of Meteorology and Geophysics, University of Innsbruck, Innsbruck, Austria

8 **Abstract**

9 We reconstruct annual glacier mass balances for 96% of the Austrian glacier covered area
10 (451 of 470 km²) between 1969 and 1998. The volume change derived from two complete
11 glacier inventories (1969 and 1998) serves as the boundary condition that we aim to
12 reproduce. ERA40 reanalysis data as well as a gridded precipitation dataset (HISTALP) are
13 used to drive a positive degree-day (PDD) model. The results are verified with four
14 independent long-term mass balance series.

15 We alter the spatial and vertical distribution of the tuning parameters in order to reproduce
16 the measured mean annual surface mass balances of selected glaciers and find a strong
17 correlation between the median elevation of a glacier and the degree-day factor (DDF) at this
18 elevation. The lower a glacier's median elevation, the less ice melt occurs at a given elevation
19 and temperature. We attribute this to the fact that lower altitude glaciers are generally in
20 regions with more winter precipitation, which leads to later exposure of bare ice and a longer
21 period of high albedo snow cover.

22 A further improvement of the model was achieved by making DDF a function of time as well
23 as space. Our results indicate that over the observation period mean DDFs generally
24 increased which probably reflects the reduction in albedo that results from a sequence of
25 consecutive negative mass balance years.

26 We finally investigate the major drivers of the observed mass balance evolution and found
27 that anomalies of summer PDD-sums correlate significantly better to the observed mass
28 balance changes than anomalies of annual PDD-sums or precipitation do.

29 **Introduction**

30 Mountain glaciers contribute considerably to observed and predicted sea level rise (e.g. Kaser
31 and others, 2006; Lemke and others, 2007; Meier and others, 2007). In order to estimate this
32 contribution, it is crucial to know glacier mass balances. Mass balance measurements are
33 restricted to few glaciers worldwide, in total around 250 glaciers (Dyurgerov and Meier,
34 2005), and only about 85 data series last longer than 10 years (Braithwaite, 2002). Most
35 glaciers for which mass balances are measured are chosen for accessibility reasons or by
36 coincidence. However, they might not be representative of the mass balances of all the
37 glaciers in a given catchment or mountain range, and simple extrapolation to other glaciers is
38 known to be unreliable (Fountain and others, 2009).

39 Different methods have been used to model the total glacier mass balance of mountain
40 ranges. Machguth and others (2009) used GCM-output to run an energy-balance model for all
41 Swiss glaciers, and Schöner and Böhm (2007) applied a statistical approach to model the
42 mass balance of a sample of Austria's glaciers as far back as the glacier maximum of the
43 Little Ice Age. Hock and others (2009) estimate the world's glaciers' total contribution to sea
44 level rise. It has also been shown that reanalysis data can be successfully used to reconstruct
45 the mass balance history of individual glaciers (e.g. Rasmussen and Wenger, 2009; Radić and
46 Hock, 2006).

47 We reconstruct the annual surface mass balance of 761 Austrian glaciers between 1969 and
48 1998, which is an important input for run-off modelling on a catchment or larger scale. We
49 show that it is necessary to use temporally and spatially varying DDFs in order to accurately
50 reproduce directly measured volume changes and their variations. Thirdly, we address the
51 generalizability of directly measured mass balances, and finally, we investigate the
52 meteorological factors that control each year's mass balance.

53 **Study Area**

54 The study area is the Austrian part of the eastern Alps (9°50' E - 13°40' E and 46°40' N -
55 47°35' N) where, in 1998, 910 glaciers covered a total area of 470 km² (Lambrecht and Kuhn,
56 2007). Fig. 1 shows a map with the glacier extent of 1998 and an ASTER Digital Elevation
57 Model (DEM) of elevations higher than 2000 m in greyscale. The ASTER DEM is used for
58 illustrative purposes only; our analysis was performed with photogrammetrically derived
59 DEMs (see Data). Mass balances have been measured over the entire modeled time span for
60 only four glaciers: Hintereisferner (HEF), Kesselwandferner (KWF), Vernagtferner (VF) and

61 Stubacher Sonnblickkees (SSK) (Schöner and Böhm, 2007). We use these glaciers (Fig. 1) to
62 validate the model and provide the basic glaciological parameters given in Tab. 1. More
63 information on the distribution of Austria's glaciers and its relationship to climate can be
64 found in Abermann and others (2010).

65 **Data**

66 Glaciological data:

67 Two glacier inventories serve as glaciological input parameters for this study. Both were
68 produced by aerial photogrammetry including glacier boundaries and DEMs (e.g. Gross,
69 1987; Lambrecht and Kuhn, 2007). Glacier area changes, which are necessary to compute
70 annual surface mass balances, are approximated by assuming that the initial area (1969)
71 remains constant until the year 1985 and then interpolating linearly to the final glacier area
72 (1998). This pattern of area change does not account for glacier growth in the late 1970s and
73 early 1980s but is similar to the mean glacier area changes of the studied period (Abermann
74 and others, 2009).

75 Volume change (ΔV) is calculated by subtracting the 1998 DEMs from the 1969 glacier
76 extent. We calculated the total balance B by

$$77 \quad B = \frac{\Delta V_{1969-1998}}{\rho} [kg \text{ or } m^3 w. e.] \quad (1)$$

78 We assume that the whole volume change has occurred as loss of ice with a density of 900
79 kgm^{-3} . We are aware of the fact that the resulting B is the upper bound of the actual volume
80 lost as some unknown fraction of the total volume change was lost as snow instead of ice. We
81 discuss this uncertainty below (see Discussion).

82 Directly measured mass balance data of four glaciers that spans the entire investigation
83 period (Tab. 1) was used to validate the model. Three of the glaciers are situated very close to
84 each other in the Ötztal valley: HEF, KWF (Kuhn and others, 1985; Hoinkes and Lang, 1962;
85 or more recently Fischer and Markl, 2008; Fischer, 2010) and VF (Reinwarth and Escher-
86 Vetter, 1999; Escher-Vetter and others, 2009). SSK (Slupetzky, 1989; Slupetzky, 2003; or
87 e.g. WGMS, 2007) is located in the Hohe Tauern and thus in a somewhat different climate
88 (Abermann and others, 2010).

89

90 Meteorological data:

91 The model takes temperature (T), equivalent-potential temperature (θ_e) and geopotential
92 height (Φ) as meteorological inputs. We use data from the 700 and 850 hPa levels of the
93 ECMWF-ERA40 reanalysis project (Uppala and others, 2005), a dynamically consistent,
94 three-dimensional, gridded dataset with a resolution of 1.25° that combines meteorological
95 and satellite observations with a numerical weather forecast model and covers the period
96 from 1957 to 2002.

97 The monthly Alps-wide precipitation dataset of the HISTALP-project has a spatial resolution
98 of $10'$ of arc and includes homogenized weather station data (Efthymiadis and others, 2006).
99 A comparison with rain gauges in high areas showed that the high Alpine precipitation is
100 strongly underestimated, which is only natural, as the dataset was generated with data from
101 valley stations only, (pers. comm. I. Auer) due to well known problems of precipitation
102 measurement at high altitudes (e.g. Frei and Schär, 1998). The general precipitation
103 anomalies tend to have similar values at high and at low altitude stations (Auer and others,
104 2005). We therefore chose to double the HISTALP-precipitation to generate reasonable
105 precipitations for high Alpine areas. We also introduced a vertical precipitation gradient of 12
106 mm/100 m/month to a maximum elevation of 3300 m, above which we did not change the
107 precipitation. This vertical gradient is larger than annual gradients given by Kuhn and others
108 (1982). Winter precipitation consists mainly of advective precipitation (unlike summer
109 precipitation, where convection plays an important role); we therefore expect larger vertical
110 gradients for winter precipitation than for annual precipitation. Since accumulation is
111 determined by winter precipitation, the chosen gradient best represented the observed vertical
112 balance profile of selected glaciers. Monthly HISTALP-precipitation values are divided up
113 into the time-steps where precipitation occurred according to ERA40 precipitation data and
114 weighted accordingly. Combining magnitudes from HISTALP with the temporal resolution
115 of ERA40 makes it possible to distinguish liquid from solid precipitation as a function of
116 elevation for each precipitation event.

117 **The Model**

118 We applied a PDD-model as widely used in hydrological modelling (e.g. Hock, 2003; Kuhn,
119 2003; Hock, 2005; Huss and others, 2008 and references therein) to calculate ablation, with

120
$$b_{abl}(x, y, z, t) = DDF(x, y, z, t) * T_{>0,day}(x, y, z, t) \text{ [mm w. e.]} \quad (2)$$

121 where DDF is used for calibration and $T_{>0,\text{day}}$ is the daily mean temperature above 0°C.

122 Accumulation is estimated by

$$123 \quad b_{\text{acc}}(x, y, z, t) = P(x, y, z, t) * R_{0/1}(x, y, z, t) \quad [\text{mm w. e.}] \quad (3)$$

124 where P is the precipitation and $R_{0/1}$ is a value that indicates whether the precipitation has
125 fallen as snow or rain and can only have the values 0 (rain) or 1 (snow). $R_{0/1}$ is determined
126 following a regression applied to observations using the equivalent potential temperature θ_e
127 (Steinacker, 1983). Liquid precipitation is assumed to not contribute to glacier mass gain.
128 Both ablation and accumulation are computed with a 6 hour timestep. Their sum gives the
129 specific mass balance b.

130 The spatial and vertical dependence of DDF is a crucial point in the model and needs
131 explanation. We first explain our approach towards the vertical dependence of DDF
132 ($d\text{DDF}/dz$), and then show how we approached $d\text{DDF}/dx$ and $d\text{DDF}/dy$.

133 The results of an energy balance model (SOMARS, for details: Greuell and Konzelmann
134 (1994)) that was applied to two locations on HEF by Schrott (2006) were used to calculate a
135 given season's mean DDF at two elevations. DDF was found to vary vertically by -0.32 mm
136 w.e./(Kd) per 100m of elevation. This 'lapse-rate' of DDFs was extrapolated and used as the
137 vertical dependence of DDF in the model. The vertically changing DDFs are in line with
138 theoretical considerations by Hock (2003). On average over a melt season, the albedo of
139 lower areas is smaller, so, for a given temperature, the energy added to a surface is higher, as
140 more shortwave radiation is absorbed. This is independent of temperature and therefore not
141 reflected in a simplified temperature-index approach.

142 In addition to the vertically varying DDFs, we introduce a spatial dependence with two
143 dimensions: $d\text{DDF}/dx$ and $d\text{DDF}/dy$. These are found by running the model iteratively with
144 $d\text{DDF}/dz$ as described above and with the condition that we must obtain the measured B of
145 each glacier as had been previously calculated from the glacier inventories. Each individual
146 glacier thus has its own set of DDFs that best represents the measured B.

147 The results of the first model run (Run I) for HEF are shown in Fig. 2a. Statistical values of
148 Tab. 2 indicate that a similar quality of results was achieved for the other glaciers where we
149 have cross-validation data (i.e. measured mass balance). Fig. 2a shows that the model
150 approximates the pattern of glacier change. There is a clear temporal dependence of the

151 differences between measured and modelled balance. Until about 1987, measured balances
152 are more positive than modelled balances, after 1987, this trend is reversed.

153 We investigated this result further by asking, which annual values do DDFs have to have on
154 average to reproduce the measured mass balance of each year? This is shown in Fig. 3 where
155 mean average DDFs are plotted over time. The average DDFs are calculated as

$$156 \quad DDF_{avg} = \frac{B_{ann,meas} - B_{acc,mod}}{\Sigma PDD} \left[\frac{m}{K \cdot d} \right]. \quad (4)$$

157 Fig. 3 shows that there is an increase in DDFs over the observation period for all glaciers for
158 which measured mass balance data exist, that is, at a given temperature, more melt occurs at
159 later points in time. The increasing trend is statistically significant and its magnitude is
160 similar for the four glaciers with complete mass balance data. The absolute values of mean
161 DDFs are largest for VF, followed closely by KWF, significantly lower for HEF and lowest
162 for SSK. For the three glaciers of the Ötztal Alps (HEF, KWF, VF), these differences are
163 likely due to the influence of shortwave radiation, as the south facing VF and southeast facing
164 KWF are expected to receive more short-wave radiation than northeast facing HEF (Tab. 1)
165 and therefore have higher DDFs, a result that is consistent with previous research (e.g. Hock,
166 2005). SSK provides a valuable comparison as well: it is located in a different climate with
167 significantly more precipitation (Abermann and others, 2010). More precipitation may cause
168 a higher mean albedo and thus lower mean DDFs. We calculated a second order polynomial
169 fit (PF) that best represents the mean of all DDF-increases and found that the overall increase
170 is approximately $1.5 \text{ mm K}^{-1} \text{d}^{-1}$ over the 29 years observed.

171 In the second model run (run II), we introduced a DDF time dependence for each glacier in
172 accordance with the findings of Fig. 3. DDF is thus a four-dimensional function of space and
173 time. Fig. 2b shows measured and modelled balances as well as their differences with
174 temporally varying DDFs for HEF. Both the trend and the amounts are better modelled than
175 in the previous run. This is also shown in Tab. 2 in the mean absolute differences (MD_{abs}),
176 mean signed differences (MD), standard deviations (STD) of the differences between
177 measured and modelled balances and the correlation coefficients (R) between measured and
178 modelled balances. With no exception, the second run gave better results; smaller MD_{abs} , MD
179 and STD, and larger R. The MD values, which are for all cases small but largest for KWF
180 (i.e. -0.17 at KWF), suggest that errors largely compensate for each other. The correlation
181 coefficients between measured and modelled balance are highest for HEF (0.85) and lowest

182 for VF (0.75) and on average 0.81. They are all quite similar, which suggests that the model
183 is applicable to glaciers of different types and that further analysis of the results is likely to be
184 well-founded.

185 **Results**

186 The results of the model run with temporally changing DDFs for all Austrian glaciers for
187 which two DEMs exist (761 out of 900 glaciers or 451 out of 470 km² or comprising 96% of
188 the total glacier area) are shown in Fig. 4, which shows the evolution of modelled cumulative
189 annual b with time for all glaciers (black lines). The wide spread of the curves is due to
190 differences in glacier type and to the individual glacier's deviation from equilibrium. The red
191 curves show the cumulative modelled b of the glaciers with directly measured mass balance,
192 and the total, area-weighted cumulative mean specific mass balance is computed and
193 displayed as a green line. Initially, the glaciers' masses remained constant. Starting in 1975,
194 all glaciers show a period of positive mass balances, with a total gain of about 1.3 m w.e.,
195 which corresponds to an ice volume gain of about 1 km³. Since 1980, only a few years (e.g.
196 1984 or 1989) interrupt the generally negative trend. This temporal sequence is in agreement
197 with the cumulative volume change derived from direct surface mass balance measurements
198 as compiled for example in Abermann and others (2009).

199 In Fig. 5 we display the set of DDFs that best reproduced the observed glacier mass loss
200 including the glacier's median elevation (location of the circles) and the mean winter
201 precipitation at the glacier (colours). Each thin line represents the DDF(z) of the run with
202 temporally constant DDFs. For the run with the changing DDFs, each line was altered with
203 time by approximately $1.5 \cdot 10^3$ m (i.e. shifted along the x-axis). There is a clear relationship
204 between the median elevation and the DDF there. The higher the median elevation, the more
205 melt generally occurs at a given temperature and given precipitation. We find two
206 explanations for this apparent paradox convincing. First, glaciers usually exist at low median
207 elevations (below 2700 m a.s.l., colours blue to yellow) because they generally accumulate
208 more mass in the winter, through greater precipitation, more wind drift, more avalanching or
209 some combination of the three. As a result, ice is kept under snow cover for a longer part of
210 the ablation season and thus the albedo is comparatively high. Second, the increasing
211 shortwave radiation with elevation results in higher general DDF values at higher elevations,
212 as suggested by Hock (2003) or Lang and Braun (1990).

213 **Discussion**

214 The dependence of DDF on time is a major challenge when attempting to model future
215 glacier change. As an example, consider the problem faced by a hypothetical modeller in
216 1975 who sought to model future glacier mass balance through 1998 using mass balance
217 records from Fig. 2 since 1969. He could not have known the future time dependence of
218 DDF, and any reasonable assumption would have resulted in a significant underestimation of
219 ice loss, as is obvious from Fig. 2.

220 The subject of temporally changing DDFs has been addressed in a recent study by Huss and
221 others (2009) who found a decrease in DDFs of approximately -7% per decade between 1970
222 and 2008. This seems to contradict the findings of this study but can be explained by the fact
223 that Huss and others (2009) calculated point mass balance, and thus DDFs, at point locations
224 that are all in the accumulation area. The increase in DDFs in our study amounts to about
225 +9% per decade and must be understood as a collective signal for an entire glacier. Since
226 mass balances in recent years have been governed by ablation, it is the ablation area and not
227 the accumulation area that controls recent average DDF change. If we were to combine the
228 findings of the two studies, it could be concluded that DDFs tend to increase over time in
229 accumulation areas (Huss and others, 2009) where surface characteristics have not changed
230 significantly, and decrease over time in ablation areas probably as a consequence of
231 sequential negative balance years and thus albedo decrease. The second process is stronger as
232 shown by the overall signal of Fig. 3. Two recent studies (Fischer, 2010; Oerlemans and
233 others, 2009) support this conclusion, attributing the recent accelerated glacier retreat partly
234 to albedo decrease.

235 This study has two important simplifications. First, we did not take into account the impact of
236 basal melt. This volume loss is reflected in measured volume changes but not in the modelled
237 surface balance as too little is known about its magnitude to accurately model it. Locally, this
238 may be an important contribution to a glacier's mass loss but on average and compared to the
239 surface mass loss we assume basal melt is negligible.

240 Our second simplification was the assumption that all volume was lost as ice. Several aerial
241 photographs were examined qualitatively indicating that a fraction of the lost volume was
242 snow. For a study of this scale, however, it was not possible to include a proportion of
243 volume lost as snow to each glacier. Therefore, to estimate the possible impact on our results,
244 we ran the model with the exaggerated assumption that half of the lost volume was snow with
245 a density of 550 kgm^{-3} . The resulting total volume loss amounts then to 0.87 km^3 w.e. less

246 than that calculated for ice. The pattern of the cumulative mass balance as well as the
247 modifications of DDF as a function of time and space do not change considerably and thus
248 the results would be altered quantitatively, but not qualitatively.

249 The results and the data presented in this study allow for an estimation of the climatic
250 influences that govern annual glacier mass balances. In Tab. 3 we summarize correlation
251 coefficients between measured balances of the four well-studied glaciers and anomalies of
252 PDD-sums for the whole year, PDD-sums for the summer (JJA), winter precipitation
253 (ONDJFMAM) and summer precipitation, all of which are interpolated to the glacier's
254 gridpoint from the HISTALP dataset. Deviations of winter and summer precipitation
255 correlate only weakly with the measured balance. Annual anomalies of PDD-sums correlate
256 much more strongly to surface mass balance than precipitation anomalies do. The strongest
257 correlation between meteorological data and measured balances is found between summer
258 anomalies of PDD-sums and the measured balance b (between -0.71 and -0.74), which is
259 consistent with the results of Kuhn and others (1999), who examined this for Hintereisferner.
260 All four glaciers have similar correlation values, but SSK shows a significantly higher
261 correlation between summer precipitation anomalies and b than the other glaciers and HEF's
262 balance is more sensitive to winter precipitation than the other glaciers'.

263 The results presented in Fig. 4 can be taken as a measurement of the generalizability of
264 measured mass balance glaciers to all Austrian glaciers. HEF is much more negative than
265 most and its b is therefore not representative for the overall mass balance of all Austrian
266 glaciers. The specific balance of VF and KWF is close to the average, while SSK's mean
267 specific balance is more positive than average.

268 **Conclusions**

269 We investigated the change over time of mean annual surface mass balance of all Austrian
270 glaciers between 1969 and 1998. With a PDD-model with DDFs that vary in space (3D) we
271 were able to reproduce the balances with correlation coefficients of more 0.8 on average. We
272 found that it is necessary to run such a model with tuning parameters calibrated to each
273 glacier individually and found a relation between the glacier's median elevation, mean winter
274 precipitation and the DDF. We found that the model results were improved by introducing a
275 long term time dependence of DDFs, specifically, a general increase over time. We suggest
276 that this is due to a larger fraction of the glacier surface that exposes bare ice and thus has a
277 lower mean albedo, which is consistent with a sequence of negative balance years and an

278 increase in equilibrium line altitude. Calibrating a PDD-model with only a few years of
279 measurements and then extrapolating to the past or future seems extremely unreliable without
280 additional knowledge (e.g. DEMs at various points in time). We are extending this study to
281 include a new glacier inventory of 2006 (Abermann and others, 2009) in order to investigate
282 how these parameters have evolved in the very recent past. This model could also be used to
283 reproduce mass balances back to the Little Ice Age glacier maximum, for which information
284 on extent and surface elevation could be reconstructed out of moraines, thus providing a
285 fascinating picture of more than 150 years of glacier history.

286 **Acknowledgements**

287 This study was funded by the Commission for Geophysical Research, Austrian Academy of
288 Science. Thanks to the Institute of Meteorology and Geophysics, Innsbruck, the Bavarian
289 Academy of Sciences, Munich and H. Slupetzky, University of Salzburg, for providing mass
290 balance data. The authors would like to thank E. Dreiseitl, E. Schlosser and S. Kinter for their
291 comments and proof-reading.

292 **References**

- 293 Abermann, J., M. Kuhn and A. Fischer. 2010. Climatic controls of glacier distribution and
294 changes in Austria. *Submitted to Annals of Glaciology*.
- 295 Abermann, J., A. Lambrecht, A. Fischer and M. Kuhn. 2009. Quantifying changes and trends
296 in glacier area and volume in the Austrian Ötztal Alps (1969-1997-2006). *The*
297 *Cryosphere*, **3**(2), 205-215.
- 298 Auer, I., R. Böhm, A. Jurkovic, A. Orlik, R. Potzmann, W. Schöner, M. Ungersböck, M.
299 Brunetti, T. Nanni, M. Maugeri, K. Briffa, P. Jones, D. Efthymiadis, O. Mestre, J.M.
300 Moisselin, M. Begert, R. Brazdil, O. Bochnicek, T. Cegnar, M. Gajic-Capka, K.
301 Zaninovic, Z. Majstorovic, S. Szalai and T. Szentimrey. 2005. A new instrumental
302 precipitation data set in the greater alpine region for the period 1800–2002.
303 *International Journal of Climatology*, **25**(2), 139-166.
- 304 Braithwaite, R.J. 2002. Glacier mass balance: the first 50 years of international monitoring.
305 *Progress in Physical Geography*, **26**(1), 90-109.
- 306 Dyurgerov, M. and M.F. Meier. 2005. Glaciers and Changing Earth System: A 2004
307 Snapshot. Occasional Paper, INSTAAR 58, University of Colorado.
- 308 Efthymiadis, D., P.D. Jones, K.R. Briffa, I. Auer, R. Böhm, W. Schöner, C. Frei and J.
309 Schmidli. 2006. Construction of a 10-min-gridded precipitation data set for the

310 Greater Alpine Region for 1800–2003. *Journal of Geophysical Research*,
311 **111**(D01105), 1-22.

312 Escher-Vetter, H., M. Kuhn and M. Weber. 2009. Four decades of winter mass balance of
313 Vernagtferner and Hintereisferner, Austria: methodology and results. *Annals of*
314 *Glaciology*, **50**, 87-95.

315 Fischer, A. 2010. Glaciers and climate change: Interpretation of 50 years of direct mass
316 balance of Hintereisferner. *Global and Planetary Change*, **71**(1-2), 13-26.

317 Fischer, A. and G. Markl. 2008. Mass balance measurements on Hintereisferner,
318 Kesselwandferner, and Jamtalferner 2003 to 2006. Database and results. *Zeitschrift*
319 *für Gletscherkunde und Glazialgeologie*, **42**(1), 47-83.

320 Fountain, A.G., M.J. Hoffman, F. Granshaw and J. Riedel. 2009. The 'benchmark glacier'
321 concept does it work? Lessons from the North Cascade Range, USA. *Annals of*
322 *Glaciology*, **50**, 163-168.

323 Frei, C. and C. Schär. 1998. A precipitation climatology of the Alps from high-resolution
324 rain-gauge observations. *International Journal of Climatology*, **18**(8), 873-900.

325 Gross, G. 1987. Der Flächenverlust der Gletscher in Österreich 1850–1920–1969. *Zeitschrift*
326 *für Gletscherkunde und Glazialgeologie*, **23**(2), 131-141.

327 Greuell, W. and T. Konzelmann. 1994. Numerical modelling of the energy balance and the
328 englacial temperature of the Greenland Ice Sheet. Calculations for the ETH-Camp
329 location (West Greenland, 1155 m a.s.l.). *Global and Planetary Change*, **9**(1-2), 91-
330 114.

331 Hock, R. 2003. Temperature index melt modelling in mountain areas. *Journal of Hydrology*,
332 **282**(1-4), 104-115.

333 Hock, R. 2005. Glacier melt: A review on processes and their modelling. *Progress in*
334 *Physical Geography*, **29**(3), 362-391.

335 Hock, R., M. de Woul, Radi, Valentina and M. Dyurgerov. 2009. Mountain glaciers and ice
336 caps around Antarctica make a large sea-level rise contribution. *Geophys. Res. Lett.*,
337 **36**(7), L07501.

338 Hoinkes, H. and H. Lang, 1962. Der Massenhaushalt von Hintereis- und Kesselwandferner
339 (Ötztaler Alpen), 1957/58 und 1958/59. *Theoretical and Applied Climatology*, **12**(2),
340 284-320.

341 Huss, M., A. Bauder, M. Funk and R. Hock. 2008. Determination of the seasonal mass
342 balance of four Alpine glaciers since 1865. *Journal of Geophysical Research*, **113**,
343 F01015.

344 Huss, M., M. Funk and A. Ohmura. 2009. Strong Alpine glacier melt in the 1940s due to
345 enhanced solar radiation. *Geophys. Res. Lett.*, **36**(23), L23501.

346 Kaser, G., J.G. Cogley, M.B. Dyurgerov, M.F. Meier and A. Ohmura. 2006. Mass balance of
347 glaciers and ice caps: Consensus estimates for 1961-2004. *Geophys. Res. Lett.*,
348 **33**(19), L19501.

349 Kuhn, M. 2003. Redistribution of snow and glacier mass balance from a hydrometeorological
350 model. *Journal of Hydrology*, **282**, 95-103.

351 Kuhn, M., E. Dreiseitl, S. Hofinger, G. Kaser, G. Markl and N. Span. 1999. Measurements
352 and Models of the Mass Balance of Hintereisferner. *Geografiska Annaler*, **81A**(4),
353 659 - 670.

354 Kuhn, M., A. Lambrecht, J. Abermann, G. Patzelt and G. Gross. 2009. *Die österreichischen*
355 *Gletscher 1998 und 1969, Flächen und Volumenänderungen*. Vienna, Austrian
356 Academy of Sciences Press.

357 Kuhn, M., G. Markl, G. Kaser, U. Nickus, F. Obleitner and H. Schneider. 1985. Fluctuations
358 of climate and mass balance: different responses of two adjacent glaciers. *Zeitschrift*
359 *für Gletscherkunde und Glazialgeologie*, **21**, 409 - 416.

360 Kuhn, M., U. Nickus and F. Pellet. 1982. Die Niederschlagsverhältnisse im inneren Ötztal.
361 *Internationale Tagung für Alpine Meteorologie*, Berchtesgaden, 235-237.

362 Lambrecht, A. and M. Kuhn. 2007. Glacier changes in the Austrian Alps during the last three
363 decades, derived from the new Austrian glacier inventory. *Annals of Glaciology*, **46**,
364 177-184.

365 Lang, H. and L. Braun. 1990. On the information content of air temperature in the context of
366 snow melt estimation. In Molnar, L., ed. *Hydrology of Mountainous Areas*,
367 *Proceedings of the Strbske Pleso Symposium 1990*, 347-354.

368 Lemke, P., J. Ren, R.B. Alley, I. Allison, J. Carrasco, G. Flato, Y. Fujii, G. Kaser, P. Mote,
369 R.H. Thomas and T. Zhang. 2007. Observations: Changes in Snow, Ice and Frozen
370 Ground. In Solomon, S., D. Qin, M. Manning, Z. Chen, M. Marquis, K.B. Averyt, M.
371 Tignor and H.L. Miller, eds. *Climate Change 2007: The Physical Science Basis*.
372 *Contribution of Working Group I to the Fourth Assessment Report of the*
373 *Intergovernmental Panel on Climate Change*, Cambridge, United Kingdom and New
374 York, NY, USA, Cambridge University Press.

375 Machguth, H., F. Paul, S. Kotlarski and M. Hoelzle. 2009. Calculating distributed glacier
376 mass balance for the Swiss Alps from regional climate model output: A methodical
377 description and interpretation of the results. *J. Geophys. Res.*, **114**(D19), D19106.

378 Meier, M.F., M.B. Dyurgerov, U.K. Rick, S. O'Neel, W.T. Pfeffer, R.S. Anderson, S.P.
379 Anderson and A.F. Glazovsky. 2007. Glaciers Dominate Eustatic Sea-Level Rise in
380 the 21st Century. *Science*, **317**(5841), 1064-1067.

381 Oerlemans, J., R.H. Giesen and M.R. Van Den Broeke. 2009. Retreating alpine glaciers:
382 increased melt rates due to accumulation of dust (Vadret da Morteratsch,
383 Switzerland). *Journal of Glaciology*, **55**, 729-736.

384 Radić, V. and R. Hock. 2006. Modeling future glacier mass balance and volume changes
385 using ERA-40 reanalysis and climate models: A sensitivity study at Storglaciären,
386 Sweden. *Journal of Geophysical Research*, **111**, F03003.

387 Rasmussen, L.A. and J.M. Wenger. 2009. Upper-air model of summer balance on Mount
388 Rainier, USA. *Journal of Glaciology*, **55**, 619-624.

389 Reinwarth, O. and H. Escher-Vetter. 1999. Mass Balance of Vernagtferner, Austria, from
390 1964/65 to 1996/97: Results for Three Sections and the Entire Glacier. *Geografiska*
391 *Annaler. Series A, Physical Geography*, **81**(4), 743-751.

392 Schöner, W. and R. Böhm. 2007. A statistical mass-balance model for reconstruction of LIA
393 ice mass for glaciers in the European Alps. *Annals of Glaciology*, **46**, 161-169.

394 Schrott, D. 2006. Flächenhafte Modellierung der Energie- und Massenbilanz am
395 Hintereisferner. (Diploma thesis, University of Innsbruck.),
396 http://imgi.uibk.ac.at/sekretariat/diploma_theses/Schrott_Daniel_2006_Dipl.pdf.

397 Slupetzky, H. 1989. Die Massenbilanzmessreihe vom Stubacher Sonnblickkees 1958/59 bis
398 1987/88. *Zeitschrift für Gletscherkunde und Glazialgeologie*, **25**(1), 69-89.

399 Slupetzky, H. 2003. Do we need long term terrestrial glacier mass balance monitoring for the
400 future? *EGS - AGU - EUG Joint Assembly*, Nice, France, 11390.

401 Steinacker, R. 1983. Diagnose und Prognose der Schneefallgrenze. *Wetter und Leben*, **35**, 81-
402 90.

403 Uppala, S.M., P.W. Kållberg, A.J. Simmons, U. Andrae, B. Da Costa, M. Fiorino, J.K.
404 Gibson, J. Haseler, A. Hernandez, G.A. Kelly, X. Li, K. Onogi, S. Saarinen, N.
405 Sokka, R.P. Allan, E. Andersson, K. Arpe, M.A. Balmaseda, A.C.M. Beljaars, L. Van
406 De Berg, J. Bidlot, N. Bormann, S. Caires, F. Chevallier, A. Dethof, M. Dragosavac,
407 M. Fisher, M. Fuentes, S. Hagemann, E. Hólm, B.J. Hoskins, L. Isaksen, P. Janssen,
408 R. Jenne, A.P. McNally, J.F. Mahfouf, J.J. Morcrette, N.A. Rayner, R.W. Saunders, P.
409 Simon, A. Sterl, K.E. Trenberth, A. Untch, D. Vasiljevic, P. Viterbo and J. Woollen.
410 2005. The ERA-40 re-analysis. *Quarterly Journal of the Royal Meteorological*
411 *Society*, **131**(612), 2961-3012.

412 WGMS. 2007. Glacier Mass Balance Bulletin No. 9 (2004-2005), *ed.* Haeberli, W., M. Zemp
 413 and M. Hoelzle. ICSU (FAGS)/IUGG(IACS)/UNEP/UNESCO/WMO, World Glacier
 414 Monitoring Service, Zurich.

415 Tables

416 **Table 1: Basic glaciological parameters for the glaciers used for validation of the model: Size,**
 417 **minimal elevation (z_{\min}), maximal elevation (z_{\max}), median elevation (z_{med}), main aspect of the**
 418 **ablation area, latitude and longitude as given in Lambrecht and Kuhn (2007) or Kuhn and**
 419 **others (2009) for 1998.**

	size [km ²]	z_{\min} [m]	z_{\max} [m]	z_{median} [m]	Exposition	lat [°]	lon [°]
HEF	8.4	2400	3710	2990	NE	46°48'	10°46'
KWF	4.2	2690	3500	3140	SE	46°51'	10°48'
VF	8.8	2760	3630	3080	SE	46°53'	10°49'
SSK	1.5	2490	3030	2760	E	47°08'	12°36'

420

421

422 **Table 2: Mean absolute difference (MD_{abs}) and the mean signed difference (MD) between**
 423 **annually measured and modelled balances, the correlation coefficient (R^2), and the standard**
 424 **deviation (STD) of the differences for two model runs (Run I: constant DDFs, Run II:**
 425 **temporally changing DDFs following the findings of Fig. 3). MD_{abs} , MD and STD are in m w.e.,**
 426 **R^2 is dimensionless.**

	Run I				Run II			
	MD_{abs}	MD	R^2	STD	MD_{abs}	MD	R^2	STD
HEF	0.31	-0.03	0.75	0.35	0.22	-0.05	0.85	0.28
KWF	0.33	-0.16	0.70	0.37	0.30	-0.17	0.80	0.35
VF	0.34	0.10	0.60	0.44	0.28	0.08	0.75	0.38
SSK	0.41	0.10	0.72	0.54	0.35	0.07	0.81	0.45

427

428

429

430

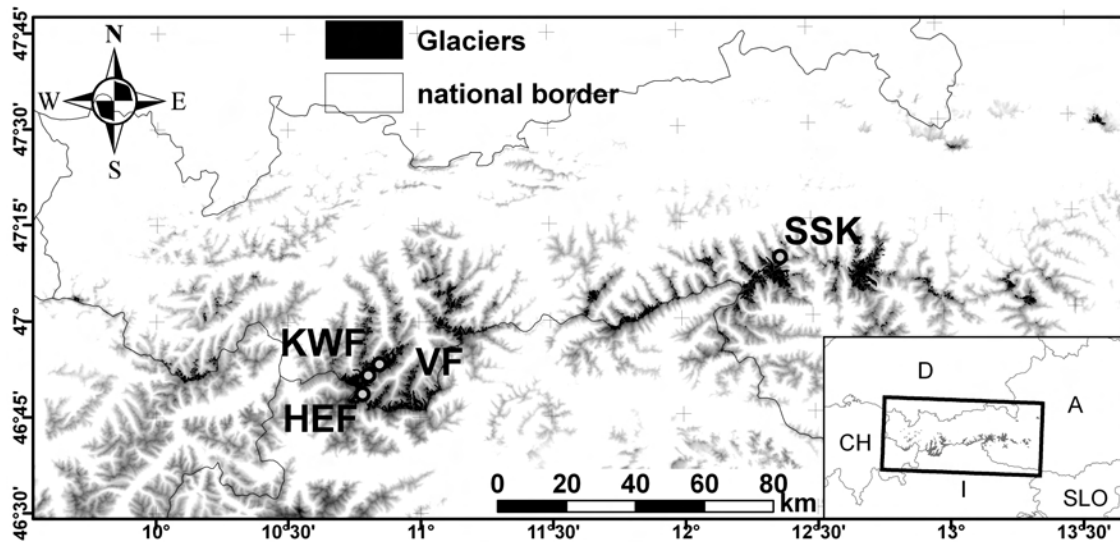
431 **Table 3: Summary of correlation coefficients of the following variables' anomalies against**
432 **measured balances: winter (october - may) (δP_{winter}) and summer (JJA) precipitation**
433 **(δP_{summer}) as well as annual ($\delta \Sigma PDD_{\text{year}}$) and summer ($\delta \Sigma PDD_{\text{summer}}$) PDD-sums. Only the last**
434 **two lines ($\delta \Sigma PDD_{\text{year}}$, $\delta \Sigma PDD_{\text{summer}}$) are statistically significant at the 99% significance level.**

	HEF	VF	KWF	SSK
δP_{winter}	0.36	0.18	0.07	0.12
δP_{summer}	0.11	0.20	0.13	0.39
$\delta \Sigma PDD_{\text{year}}$	-0.66	-0.66	-0.59	-0.71
$\delta \Sigma PDD_{\text{summer}}$	-0.72	-0.69	-0.74	-0.78

435

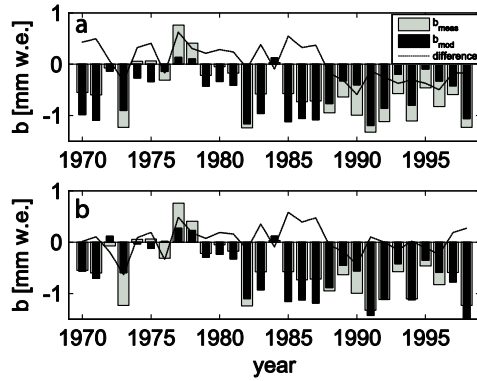
436

437 **Figures**



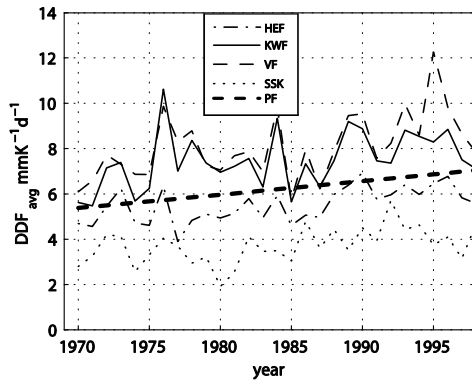
438

439 **Figure 1: Glacier cover in Austria according to the glacier inventory of 1998 (Lambrecht and**
440 **Kuhn, 2007). The glaciers HEF, KWF, VF and SSK are marked and an ASTER DEM in the**
441 **background displaying elevations higher than 2000 m in a grey-scale.**



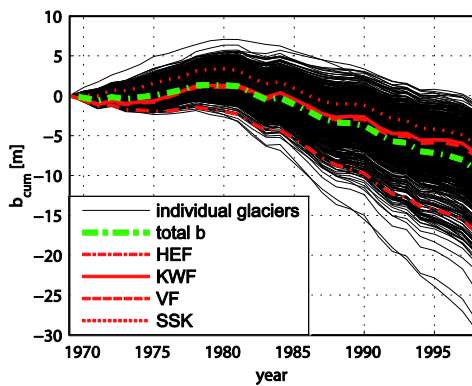
442

443 **Figure 2: Measured and modelled mean specific surface mass balance b at HEF for two**
 444 **different model runs. Fig. 2a is calculated with constant DDFs over time, in Fig 2b, a temporally**
 445 **rising DDF-value is introduced based on findings of Fig.3.**



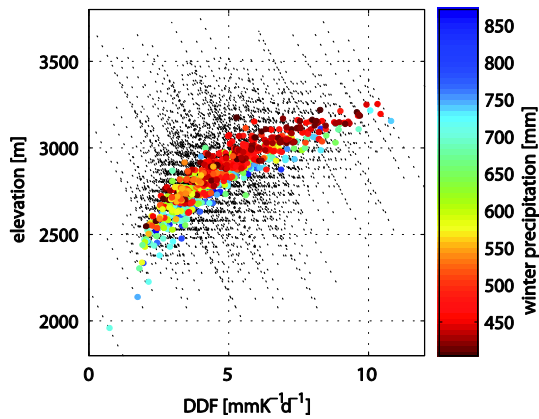
446

447 **Figure 3: Mean area and elevation weighed DDF that reproduces best the measured annual**
 448 **surface mass balance of HEF, KWF, VF and SSK as calculated according to eq. 4. PF is the**
 449 **polynomial second order fit that is calculated in order to represent the mean of the glacier's**
 450 **individual values.**



451

452 **Figure 4: Cumulative mean specific surface mass balance of all Austrian glaciers for which**
453 **volume change data exist (black lines). The red lines show modelled balances of the glaciers**
454 **where direct mass balance measurements exist. The blue line refers to the right ordinate and**
455 **shows the cumulative volume change of all Austrian glaciers.**



456

457 **Figure 5: DDF as a function of elevation for each glacier (thin dashed lines). The colour of the**
458 **dots show the mean winter precipitation at the glacier's coordinate according to HISTALP**
459 **(October – May, colour scale), their location the DDF at the glacier's median elevation (left**
460 **scale).**